

1-4 丁炔二醇和乙二胺对离子液体电沉积 Cu 的影响

燕 波 张锦秋 杨培霞 安茂忠*

(城市水资源与水环境国家重点实验室, 哈尔滨工业大学化工学院, 哈尔滨 150001)

摘要: 研究了 1-4 丁炔二醇和乙二胺作为添加剂对在离子液体 1-甲基-3-甲基咪唑三氟甲磺酸盐中电沉积 Cu 的影响。紫外可见光吸收光谱结果表明, 当采用 1-4 丁炔二醇作为添加剂时, 1-4 丁炔二醇吸附在工作电极表面且未与溶液中的 Cu^{2+} 形成配合物。扫描电镜测试结果表明由于 1-4 丁炔二醇与离子液体的正离子的竞争吸附使得 Cu 的沉积电势发生正移并使镀层表面更加均匀平整。当采用乙二胺作为添加剂时, 紫外可见光吸收光谱和循环伏安测试结果表明乙二胺与溶液中的 Cu^{2+} 离子形成带有正电荷的络合离子使得 Cu 的沉积电势发生正移, 扫描电镜和原子力显微镜测试结果表明得到了更加均匀的镀层。当同时加入 1-4 丁炔二醇和乙二胺时, Cu 的沉积电势仍然发生正移并得到具有纳米粒径的镀层。

关键词: 添加剂; 离子液体; 电沉积; Cu 镀层

中图分类号: O614.121; TQ47.1; TQ153.1

文献标识码: A

文章编号: 1001-4861(2014)04-0952-09

DOI: 10.11862/CJIC.2014.121

Effect of 2-Butyne-1,4-diol and Ethylene Diamine on Electrodeposition of Cu from Ionic Liquid

YAN Bo ZHANG Jin-Qiu YANG Pei-Xia AN Mao-Zhong*

(State Key Laboratory of Urban Water Resource and Environment, School of Chemical Engineering and Technology, Harbin Institute of Technology, Harbin 150001, China)

Abstract: The effect of additives, 2-Butyne-1,4-diol (BDO) and ethylene diamine (EDA), was investigated on the electrodeposition of Cu from 1-hexyl-3-methylimidazolium trifluoromethanesulfonate ([HMIM]OTf). The results of UV-Vis absorption spectra and Cyclic voltammograms indicate that the reduction potential of Cu shifts to the positive side with the addition of BDO without any changes in the coordination environment of Cu^{2+} . The adsorption of BDO on surface of working electrode results in a change in morphology of the obtained deposit. In the presence of EDA, the coordination environment of Cu^{2+} is changed, suggesting the formation of a new complex by Cu^{2+} and EDA. The deposition potential shifts to the positive side with addition of EDA. Scanning electron microscope and atomic force microscope tests show that the surface morphology of the obtained deposit is flatter and more granular compared to that without EDA. When BDO and EDA are added into [HMIM]OTf at the same time, the deposition potential still shifts positively and nano-sized grains are obtained.

Key words: ionic liquid; 2-butyne-1,4-diol; ethylene diamine; electrodeposition; Cu

Room temperature ionic liquids (RTILs) are expected as a new electrodepositing bath for their wide electrochemical window (usually 3.8~4.4 V vs

Pt), low vapor pressure (often between 10^{-9} and 10^{-8} Pa at room temperature), high ionic conductivity and excellent thermal stability^[1-4]. Thus, RTILs have been

收稿日期: 2013-11-01。收修改稿日期: 2013-12-09。

国家自然科学基金(No.51074057)资助项目。

*通讯联系人。E-mail: mzan@hit.edu.cn

widely used for electrodeposition of metals and alloys, especially for active metals difficult to be deposited from aqueous system. Many groups have investigated electrodepositing metals from different kinds of ionic liquids. Yi-Ting Hsieh et al.^[5-6] electro-deposited hexagonal hollow copper-tin tube arrays and hierarchical single crystalline copper-tin nanobrushes from 1-ethyl-3-methylimidazolium dicyanamide ionic liquid. Zein El Abedin et al.^[7] successfully electrode-positated nano-crystalline aluminium from the Lewis acidic ionic liquid based on AlCl_3 (60mol%) and 1-(2-methoxyethyl)-3-methylimidazolium chloride ([MoeMIm]Cl) (40mol%). Gasparotto et al.^[8] investigated the under potential deposition of Li on Au(111) from an air- and water-stable ionic liquid 1-butyl-1-methylpyrrolidinium bis (trifluoromethylsulfonyl)amide ([BMP][TFSI]). Osamu Shimamura et al.^[9] reported electrochemical co-deposition of magnesium with lithium from *N,N*-diethyl-*N*-methyl-*N*-(2-methoxyethyl) ammonium bis (trifluoromethylsulfonyl)imide ([DEME][TFSI]) and found that Mg cannot be deposited from the used ionic liquid but can be codeposited with Li.

Additives play an important role in electrodeposition. Most additives in aqueous solution affect the deposition in two different ways: (a) the additives adsorb on the surface of the electrode and alter the electrochemical double layer, inhibiting the nucleation of metal at the beginning of deposition; (b) the additives ligate the metal ions and form a complex which is more stable and more difficult to be reduced. However, as the difference of electrochemical double layer between ionic liquid and aqueous solution, the traditional models of electrochemical double layer are not suitable for ionic liquids^[10-11]. Thus it is difficult to investigate the effect of additives on electrodeposition from ionic liquids. Relatively few studies focused on the effect of additives in ionic liquid. Andrew P. Abbott et al.^[12] reported that adding ethylene diamine into 1:2 CHCl_3 :ethylene glycol containing $0.3 \text{ mol} \cdot \text{dm}^{-3}$ ZnCl_2 would promote the reduction of Zn by reducing the activity of free chloride ions close to the electrode surface. Ryuta Fukui et al. found that the coordination environment of Co^{2+} in 1-butyl-1-methylpyrrolidinium

bis (trifluoromethylsulfonyl)amide changed from $[\text{Co}(\text{TfSA})_3]^-$ to $[\text{Co}(\text{TU})_4]^{2+}$ by adding thiourea into electrolyte which making the reduction potential of Co^{2+} move to a more positive potential^[13].

Electrodeposition of Cu from aqueous solution has been widely studied in the past decades and various kinds of additives have been used to obtain a dense and bright Cu film^[14-19]. However, relatively few studies focus on the effect of additives on the electrodeposition of Cu from ionic liquids since the same additive may effect in different way in ionic liquids compared to aqueous solution^[20]. 2-Butyne-1,4-diol (BDO) is widely used in electrodeposition as an additive and ethylene diamine (EDA) is commonly used as a complexing agent in electrodeposition of Cu. In the present work, deposition of Cu from 1-hexyl-3-methylimidazolium trifluoromethanesulfonate ionic liquid was studied and 2-butyne-1,4-diol and ethylene diamine were used as additives. Furthermore, their effect on the electrodeposition mechanism and the resulting deposit morphology was described.

1 Experimental

1.1 Chemical and reagents

The ionic liquid 1-hexyl-3-methylimidazolium trifluoromethanesulfonate ([HMIM][OTF]) (Shanghai Chengjie Chemical Co., Ltd.) was chosen for the deposition of Cu due to its wider electrochemical window and good solubility for Cu ions. [HMIM][OTF] was dried under vacuum for 24 h at 373 K. Anhydrous $\text{Cu}(\text{CF}_3\text{SO}_3)_2$ (Sigma-Aldrich, 99%) was dissolved in [HMIM][OTF] to prepare the electrolyte. The electrolyte was then stirred for 24 h at 333 K before electrodeposition or electrochemical tests. 2-Butyne-1,4-diol (Sigma-Aldrich, 99%) and ethylene diamine (Sigma-Aldrich, 99%) were separately added to the Cu electroplating bath and then the electrolyte was stirred until a homogeneous liquid was formed.

1.2 Measurement procedures and apparatus

In a conventional 3-electrode cell, a copper foil with 1 cm^2 working area, a copper foil and a platinum wire were used as the working electrode (WE), the counter electrode (CE) and the quasireference

electrode (QRE), respectively. Cyclic voltammograms (CVs) and potentiostatic electrolysis were carried out using a Princeton Applied Research Parstat 2273 potentiostat/galvanostat controlled by PowerSuite software. All the electrochemical experiments were carried out in an argon gas-filled 3-electrode cell with concentration of O_2 and $H_2O < 10 \mu L \cdot L^{-1}$. The electrolyte was prepared under air and a bottle cap with three Cu wires in it was used to sealing the electrolyte. The working electrode, counter electrode and quasireference electrode were hanged with Cu wires, respectively. Electrolyte and bottle cap were put into glovebox together and then the electrolyte was capped and taken out of the glovebox so the concentration of O_2 and H_2O in 3-electrode cell was lower than $10 \mu L \cdot L^{-1}$.

A field-emission scanning electron microscope (FE-SEM, Hitachi S4700) was used to characterize the surface morphologies of the deposit. The absorption of ionic liquid containing $0.1 \text{ mol} \cdot L^{-1} Cu(CF_3SO_3)_2$, $0.1 \text{ mol} \cdot L^{-1} Cu(CF_3SO_3)_2 + 0.001 \text{ mol} \cdot L^{-1} BDO$ and $0.1 \text{ mol} \cdot L^{-1} Cu(CF_3SO_3)_2 + 0.001 \text{ mol} \cdot L^{-1} EDA$ were measured using an air-tight quartz cell (light path length 1 mm) with the aid of UV-Vis spectrometer (Shimazu, UV-2550). Atomic force microscope (AFM) was employed to study the surface roughness of the Cu deposits. The AFM analysis was carried out with a Dimension Icon (Bruker), working in contact mode with silicon nitride cantilevers.

2 Results and discussion

In order to study the coordination environment of Cu ions in ionic liquid, the absorption of ionic liquid containing $0.1 \text{ mol} \cdot L^{-1} Cu(CF_3SO_3)_2$ and $0.1 \text{ mol} \cdot L^{-1} Cu(CF_3SO_3)_2 + 0.001 \text{ mol} \cdot L^{-1} BDO$ were measured. Fig. 1a and b represents the UV-Vis absorption spectra of ionic liquid containing $0.1 \text{ mol} \cdot L^{-1} Cu(CF_3SO_3)_2$ and the UV-Vis absorption spectra of ionic liquid containing $0.1 \text{ mol} \cdot L^{-1} Cu(CF_3SO_3)_2 + 0.001 \text{ mol} \cdot L^{-1} BDO$, respectively. The color of electrolyte changes from colorless to light green after the addition of Cu^{2+} ions. Since the base line is neat ionic liquid, the absorption peak around 800 nm in Fig.1a should be

due to the addition of Cu^{2+} ions into ionic liquid. The color of electrolyte containing $0.1 \text{ mol} \cdot L^{-1} Cu^{2+}$ ions still keeps light green after adding $0.001 \text{ mol} \cdot L^{-1} BDO$ and no difference is found between the spectra before and after the addition of BDO, indicating that the coordination environment of Cu^{2+} ions in [HMIM]OTF stays the same with the addition of BDO. And BDO might be adsorbed on the surface of electrode.

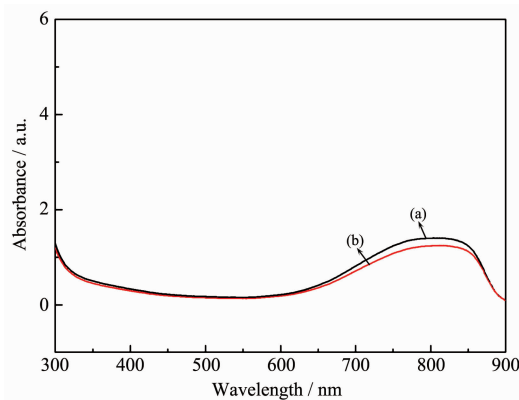


Fig.1 UV-Vis absorption spectra obtained in [HMIM] OTF containing (a) $0.1 \text{ mol} \cdot L^{-1} Cu(CF_3SO_3)_2$ and (b) $0.1 \text{ mol} \cdot L^{-1} Cu(CF_3SO_3)_2 + 0.001 \text{ mol} \cdot L^{-1} BDO$

The reduction process of Cu^{2+} to Cu is commonly recognized that Cu^{2+} is reduced to Cu^+ firstly and then Cu^+ is reduced to $Cu^{[21]}$. The activation energy of monovalent ions accepting electron is much smaller than that of divalent ions. In the reduction reaction of Cu^{2+} to Cu, the control step is $Cu^{2+} \rightarrow Cu^+$ and Cu^+ is easily reduced to Cu. A two-step two-electron reduction of Cu^{2+} to Cu is studied in *N*-butyl-*N*-methylpyrrolidinium bis (trifluoromethylsulfonyl)imide ionic liquid ([BMP][TFSI]). However, only one reduction peak at about -0.4 V (vs Pt) is detected in [HMIM]OTF containing $0.1 \text{ mol} \cdot L^{-1} Cu(CF_3SO_3)_2$ and the oxidation process starts from -0.25 V and then ends when the scan potential switches to negative, as shown in Fig. 2a, indicating that not only the deposited Cu but also the Cu substrate is stripped. Interestingly, a two-step two-electron reduction of Cu^{2+} to Cu is detected when a Pt foil is used as WE (working electrode), as shown in the inset of Fig.2, which may be due to the different reduction overpotential of Cu^{2+} ions on different substrates. Mostly, metal ions are easily deposited when the used WE has similar crystal lattice. When

the CVs of [HMIM]OTF containing $0.1 \text{ mol} \cdot \text{L}^{-1}$ $\text{Cu}(\text{CF}_3\text{SO}_3)_2$ are carried out on Cu electrode, Cu^+ is easily reduced to Cu which makes it difficult to distinguish from the reduction process of Cu^{2+} to Cu^+ . Thus only one reduction peak is detected.

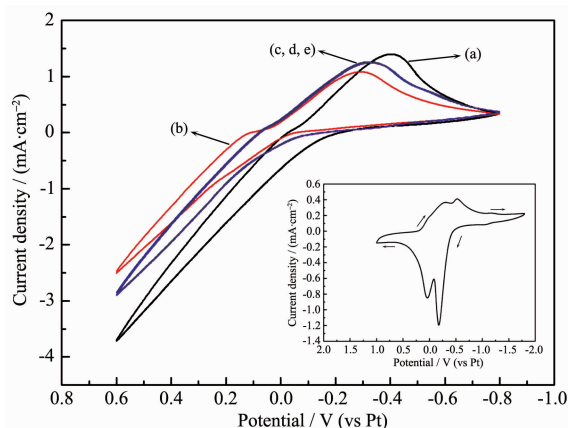


Fig.2 (a) CVs on Cu WE in [HMIM]OTF containing $0.1 \text{ mol} \cdot \text{L}^{-1}$ $\text{Cu}(\text{CF}_3\text{SO}_3)_2$, (b) $0.1 \text{ mol} \cdot \text{L}^{-1}$ $\text{Cu}(\text{CF}_3\text{SO}_3)_2$ + $0.001 \text{ mol} \cdot \text{L}^{-1}$ BDO, (c) $0.1 \text{ mol} \cdot \text{L}^{-1}$ $\text{Cu}(\text{CF}_3\text{SO}_3)_2$ + $0.003 \text{ mol} \cdot \text{L}^{-1}$ BDO, (d) $0.1 \text{ mol} \cdot \text{L}^{-1}$ $\text{Cu}(\text{CF}_3\text{SO}_3)_2$ + $0.005 \text{ mol} \cdot \text{L}^{-1}$ BDO and (e) $0.1 \text{ mol} \cdot \text{L}^{-1}$ $\text{Cu}(\text{CF}_3\text{SO}_3)_2$ + $0.007 \text{ mol} \cdot \text{L}^{-1}$ BDO; Inset shows the cyclic voltammogram on a Pt electrode in [HMIM]OTF containing $0.1 \text{ mol} \cdot \text{L}^{-1}$ $\text{Cu}(\text{CF}_3\text{SO}_3)_2$; Scan rate: $10 \text{ mV} \cdot \text{s}^{-1}$; Temperature: 333 K

It is clear from Fig.2b that the presence of the BDO causes significant changes in the position of the voltammograms. The reduction potential of Cu^{2+} is shifted anodically by almost 150 mV to $E = -0.27 \text{ V}$ after adding $0.001 \text{ mol} \cdot \text{L}^{-1}$ BDO into electrolyte and the oxidation potential also shifts slightly to a more positive potential at about 0 V , suggesting that the presence of BDO acts to promote the reduction of Cu and alters both the Cu deposition and stripping process although the coordination environment of Cu^{2+} is expected to be identical in both absence and presence of BDO. The decrease in the overpotential of electrodeposition of Cu may be explained by a decrease in the coverage of HMIM⁺ on the surface of the substrate. BDO is widely used in electrodeposition as leveler which adsorbs on the surface of the cathode and increases the overpotential of electrodeposition. However, in the present work BDO shows an opposite effect to that observed for Ni^[22]. The slight decrease in

the overpotential in this ionic liquid may be related to the change of the structure of electric double layer^[23]. Some researchers pointed out that bulky cations may adsorb on the surface of the cathode and prevent the reduction process of metal ions^[24-26]. When adding $0.001 \text{ mol} \cdot \text{L}^{-1}$ BDO into electrolyte, it is possible that the electrode reaction becomes more favorable by replacement of adsorbed bulky cations with smaller molecules, such as BDO, which have higher adsorbing ability than the cations. After increasing the concentration of BDO to $0.003 \text{ mol} \cdot \text{L}^{-1}$, the reduction potential of Cu^{2+} moves negatively by almost 50 mV to $E = -0.32 \text{ V}$. It is rather reasonable for the negative moving of reduction potential of Cu although the addition of BDO decreases the overpotential of Cu compared to the electrolyte without BDO. When increasing the concentration of BDO, more and more BDO molecules adsorb on the surface of electrode which may prevent the electrode reaction processes, such as electron transfer, surface diffusion and crystalline growth. Therefore, the deposition of Cu becomes more difficult. However, when continue increasing the concentration of BDO to $0.005 \text{ mol} \cdot \text{L}^{-1}$, the reduction potential of Cu^{2+} stays the same as that for the BDO concentration of $0.003 \text{ mol} \cdot \text{L}^{-1}$, suggesting that the adsorption of BDO does not always increase with the increasing concentration of BDO but remains at a certain degree.

Fig.3 contains SEM images of the electrodeposits obtained by a potentiostatic electrolysis on Cu substrate in [HMIM]OTF containing $0.1 \text{ mol} \cdot \text{L}^{-1}$ $\text{Cu}(\text{CF}_3\text{SO}_3)_2$ with (a) 0, (b) 0.001 , (c) $0.003 \text{ mol} \cdot \text{L}^{-1}$ BDO and AFM three-dimensional height images of the copper deposit obtained by a potentiostatic electrolysis on Cu substrate in [HMIM]OTF containing $0.1 \text{ mol} \cdot \text{L}^{-1}$ $\text{Cu}(\text{CF}_3\text{SO}_3)_2$ with (d) 0, (e) 0.001 and (f) $0.003 \text{ mol} \cdot \text{L}^{-1}$ BDO. In the absence of BDO (Fig.3a) Cu deposited from [HMIM]OTF presents a two-dimensional layered morphology, which is quite different from Cu deposits obtained from aqueous solution. This two-dimensional layered morphology may be caused by the adsorption of HMIM⁺ on the surface of electrode. As shown in Fig.3b, the addition

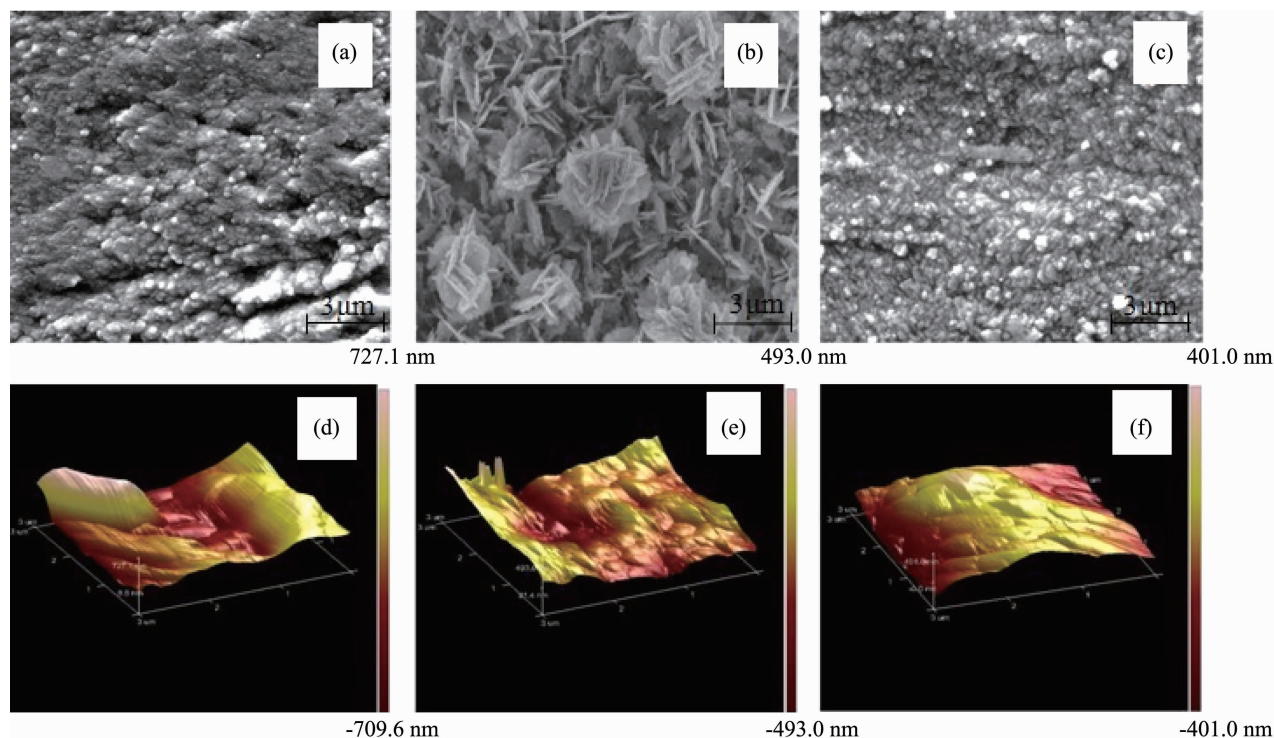


Fig.3 SEM images of the electrodeposits obtained by a potentiostatic electrolysis on Cu substrate in [HMIM]OTF containing $0.1 \text{ mol} \cdot \text{L}^{-1} \text{ Cu}(\text{CF}_3\text{SO}_3)_2$ with (a) 0, (b) 0.001, (c) $0.003 \text{ mol} \cdot \text{L}^{-1}$ BDO and AFM images of the electrodeposit obtained by a potentiostatic electrolysis on Cu substrate in [HMIM]OTF containing $0.1 \text{ mol} \cdot \text{L}^{-1} \text{ Cu}(\text{CF}_3\text{SO}_3)_2$ with (d) 0, (e) 0.001 and (f) $0.003 \text{ mol} \cdot \text{L}^{-1}$ BDO; All electrodepositions were carried out on Cu plates at 333 K and under a deposition potential of -0.4 V for 2 h

of $0.001 \text{ mol} \cdot \text{L}^{-1}$ BDO leads to a change in morphology. BDO is a typical leveler, which alters the morphology of electrodeposits effectively at a very low concentration by the adsorption of the leveler on the surface of the electrode. When adding $0.001 \text{ mol} \cdot \text{L}^{-1}$ BDO, the adsorption of BDO replaces the adsorption of HMIM^+ which makes it easier for the nucleation process of Cu^{2+} ions. Therefore, the appearance of the deposits obtained with BDO is more granular and smoother than that without BDO. With the increasing concentration of BDO, the deposits becomes more granular indicating that the formation of new nucleation is more favorable than the growth of existing Cu crystallites.

As shown in Fig.3d, in the absence of BDO the morphology of the obtained deposit is uneven and coarse. Checked by NanoScope Analysis, the Ra (Average roughness) is 202 nm while Rq (Root Mean Square (Rms) roughness) is 262 nm. After the addition of $0.001 \text{ mol} \cdot \text{L}^{-1}$ BDO, the surface of the

obtained deposit becomes smoother and Ra decreases to 115 nm when Rq decreases to 139 nm at the same time. With the increasing concentration of BDO, the morphology of the obtained deposit becomes much smoother and Ra further decreases to 88.5 nm while Rq decreases to 120 nm, indicating that the addition of BDO smoothens the morphology of the obtained deposit.

EDA is commonly used as a complexing agent in electrodeposition of Cu due to its strong hydrogen bond for formation of more stable complexes with Cu^{2+} ions such as $[\text{Cu}(\text{EDA})]^{2+}$ and $[\text{Cu}(\text{EDA})_2]^{2+}$ in aqueous solutions^[27]. The color of the [HMIM]OTF containing $0.1 \text{ mol} \cdot \text{L}^{-1} \text{ Cu}^{2+}$ changes from light green to navy blue due to the addition of EDA, suggesting the change in the coordination environment of Cu^{2+} . However, it is difficult to determining speciation in ionic liquids since there is no possibility to evaporate the solvent to leave the metal complex. Fig.4 shows the UV-Vis absorption of [HMIM]OTF containing $0.001 \text{ mol} \cdot \text{L}^{-1}$

EDA, $0.1 \text{ mol} \cdot \text{L}^{-1} \text{ Cu}(\text{CF}_3\text{SO}_3)_2$ and $0.1 \text{ mol} \cdot \text{L}^{-1} \text{ Cu}(\text{CF}_3\text{SO}_3)_2 + 0.001 \text{ mol} \cdot \text{L}^{-1} \text{ EDA}$ at room temperature. No absorption peak was detected when adding $0.001 \text{ mol} \cdot \text{L}^{-1} \text{ EDA}$ to [HMIM]OTF, indicating that no reaction happens between [HMIM]OTF and EDA. After adding $0.1 \text{ mol} \cdot \text{L}^{-1} \text{ Cu}$ to [HMIM]OTF the color of the electrolyte changes from colorless to light green and a broad absorption peak around 800 nm is detected, as shown in Fig.4b. When $0.001 \text{ mol} \cdot \text{L}^{-1} \text{ EDA}$ is added into ionic liquid, the absorption peak shifts negatively to 600 nm , indicating that new complex is formed by Cu^{2+} and EDA. The change in the position of absorption peak is not derived from EDA itself, as shown in Fig.4a.

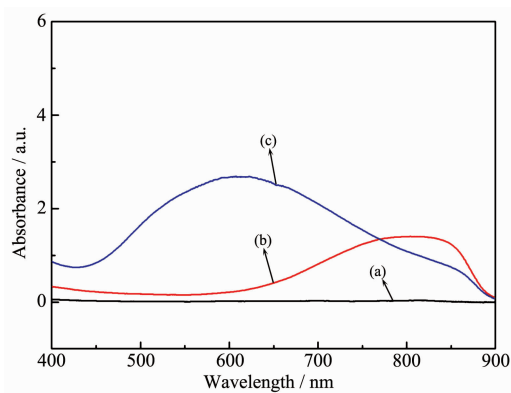


Fig.4 UV-Vis absorption spectra obtained in [HMIM]OTF containing (a) $0.001 \text{ mol} \cdot \text{L}^{-1} \text{ EDA}$, (b) $0.1 \text{ mol} \cdot \text{L}^{-1} \text{ Cu}(\text{CF}_3\text{SO}_3)_2$ and (c) $0.1 \text{ mol} \cdot \text{L}^{-1} \text{ Cu}(\text{CF}_3\text{SO}_3)_2 + 0.001 \text{ mol} \cdot \text{L}^{-1} \text{ EDA}$

Fig.5 shows the CVs of [HMIM]OTF containing $0.1 \text{ mol} \cdot \text{L}^{-1} \text{ Cu}(\text{CF}_3\text{SO}_3)_2$, $0.1 \text{ mol} \cdot \text{L}^{-1} \text{ Cu}(\text{CF}_3\text{SO}_3)_2 + 0.001 \text{ mol} \cdot \text{L}^{-1} \text{ EDA}$, $0.1 \text{ mol} \cdot \text{L}^{-1} \text{ Cu}(\text{CF}_3\text{SO}_3)_2 + 0.003 \text{ mol} \cdot \text{L}^{-1} \text{ EDA}$, $0.1 \text{ mol} \cdot \text{L}^{-1} \text{ Cu}(\text{CF}_3\text{SO}_3)_2 + 0.005 \text{ mol} \cdot \text{L}^{-1} \text{ EDA}$ and $0.1 \text{ mol} \cdot \text{L}^{-1} \text{ Cu}(\text{CF}_3\text{SO}_3)_2 + 0.007 \text{ mol} \cdot \text{L}^{-1} \text{ EDA}$ on Cu electrode. Interestingly, two reduction peaks are detected with the addition of $0.001 \text{ mol} \cdot \text{L}^{-1} \text{ EDA}$ while only one reduction peak is detected in the absence of EDA, indicating that a two-step two-electron reduction process of Cu^{2+} happens in the presence of EDA. The two reduction peaks at about -0.28 and -0.58 V in Fig.5b suggesting the reduction process of Cu^{2+} to Cu^+ and Cu^+ to Cu , respectively. As described above, in aqueous solutions EDA will form a more stable complex with Cu^{2+} instead of aqua-

complex. In case of [HMIM]OTF, EDA may form similar complex with Cu^{2+} ions, such as $[\text{Cu}(\text{EDA})]^{2+}$ or $[\text{Cu}(\text{EDA})_2]^{2+}$. The newly formed complex may be expected more stable thermodynamically than the complex formed by Cu^{2+} and CF_3SO_3^- . However, the overpotential for Cu deposition is considered to be affected by both the speciation in ionic liquids and the structure of electroic double layer^[23]. In the presence of EDA, the newly formed complex with positive charge is expected to covering on the surface of electrode, which makes it easier for the reduction process of Cu^{2+} to Cu^+ under a comparatively negative potential, as shown in the positive shift in the reduction potential of Cu^{2+} to Cu^+ in Fig.5b. When increasing the concentration of EDA to $0.003 \text{ mol} \cdot \text{L}^{-1}$, both the reduction potential of Cu^{2+} and Cu^+ are almost the same as the electrolyte with $0.001 \text{ mol} \cdot \text{L}^{-1} \text{ EDA}$. When continue increasing the concentration of EDA, the reduction potential of Cu^{2+} stays the same as the concentration of EDA is $0.003 \text{ mol} \cdot \text{L}^{-1}$.

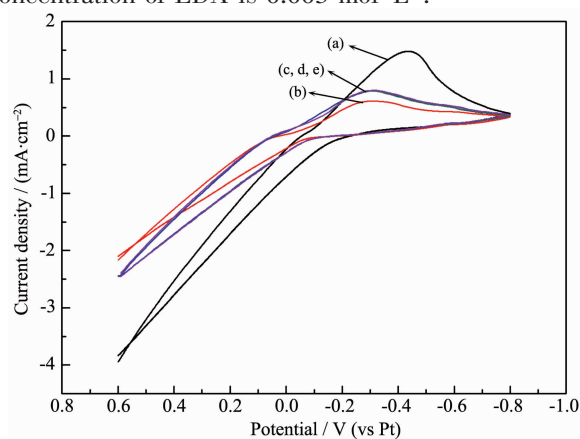


Fig.5 (a) CVs on Cu WE in [HMIM]OTF containing $0.1 \text{ mol} \cdot \text{L}^{-1} \text{ Cu}(\text{CF}_3\text{SO}_3)_2$, (b) $0.1 \text{ mol} \cdot \text{L}^{-1} \text{ Cu}(\text{CF}_3\text{SO}_3)_2 + 0.001 \text{ mol} \cdot \text{L}^{-1} \text{ EDA}$, (c) $0.1 \text{ mol} \cdot \text{L}^{-1} \text{ Cu}(\text{CF}_3\text{SO}_3)_2 + 0.003 \text{ mol} \cdot \text{L}^{-1} \text{ EDA}$, (d) $0.1 \text{ mol} \cdot \text{L}^{-1} \text{ Cu}(\text{CF}_3\text{SO}_3)_2 + 0.005 \text{ mol} \cdot \text{L}^{-1} \text{ EDA}$ and (e) $0.1 \text{ mol} \cdot \text{L}^{-1} \text{ Cu}(\text{CF}_3\text{SO}_3)_2 + 0.007 \text{ mol} \cdot \text{L}^{-1} \text{ EDA}$; Scan rate: $10 \text{ mV} \cdot \text{s}^{-1}$; Temperature: 333 K

Fig.6 gives SEM images of the deposits obtained by a potentiostatic electrolysis on Cu substrate in [HMIM]OTF containing $0.1 \text{ mol} \cdot \text{L}^{-1} \text{ Cu}(\text{CF}_3\text{SO}_3)_2$ with 0, 0.001 and $0.003 \text{ mol} \cdot \text{L}^{-1} \text{ EDA}$ and AFM three-dimensional height images of the copper deposit also obtained by a potentiostatic electrolysis on Cu

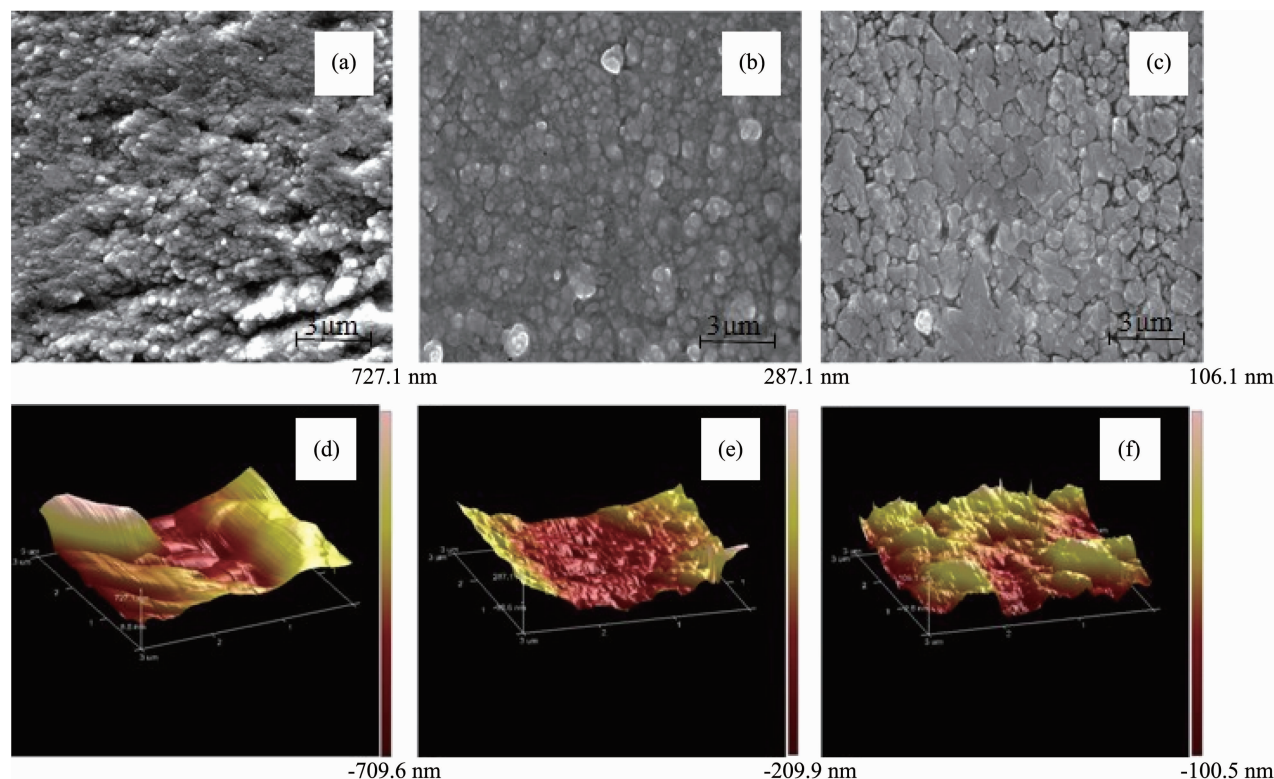


Fig.6 SEM images of the electrodeposits obtained by a potentiostatic electrolysis on Cu substrate in [HMIM]OTF containing $0.1 \text{ mol} \cdot \text{L}^{-1} \text{ Cu}(\text{CF}_3\text{SO}_3)_2$ with (a) 0, (b) 0.001, (c) $0.003 \text{ mol} \cdot \text{L}^{-1}$ EDA and AFM images of the electrodeposit obtained by a potentiostatic electrolysis on Cu substrate in [HMIM]OTF containing $0.1 \text{ mol} \cdot \text{L}^{-1} \text{ Cu}(\text{CF}_3\text{SO}_3)_2$ with (d) 0, (e) 0.001 and (f) $0.003 \text{ mol} \cdot \text{L}^{-1}$ EDA; All electrodepositions were carried out on Cu plates at 333 K and under a deposition potential of -0.4 V for 2 h

substrate in [HMIM]OTF containing $0.1 \text{ mol} \cdot \text{L}^{-1} \text{ Cu}(\text{CF}_3\text{SO}_3)_2$ with 0, 0.001 and $0.003 \text{ mol} \cdot \text{L}^{-1}$ EDA. In the presence of EDA, the obtained deposit is flatter and more granular, which may be caused by the covering of newly formed complex with positive charge on the surface of electrode. When increasing the concentration of EDA to $0.003 \text{ mol} \cdot \text{L}^{-1}$, the obtained grain is bigger than that obtained from the electrolyte with $0.001 \text{ mol} \cdot \text{L}^{-1}$ EDA, indicating that the increasing of concentration of EDA may be favorable for the growth of existing Cu crystallites.

Fig.6e and Fig.6f show that the presence of EDA makes the morphology of the obtained deposit smoother and less coarse. Checked by NanoScope Analysis, Ra decreases to 65.8 nm when Rq decreases to 79.3 nm at the same time. Although the grain size is getting bigger with the increasing concentration of EDA, Ra further decreases to 22.9 nm while Rq decreases to 28.9 nm, indicating that the morphology

of the obtained deposit is much smoother.

Most traditional electrolytes for deposition always contain different types of additives. For further studies, $0.003 \text{ mol} \cdot \text{L}^{-1}$ BDO and $0.003 \text{ mol} \cdot \text{L}^{-1}$ EDA were added to [HMIM]OTF containing $0.1 \text{ mol} \cdot \text{L}^{-1} \text{ Cu}^{2+}$ at the same time. CV of [HMIM]OTF containing $0.1 \text{ mol} \cdot \text{L}^{-1} \text{ Cu}(\text{CF}_3\text{SO}_3)_2$, $0.003 \text{ mol} \cdot \text{L}^{-1}$ BDO and $0.003 \text{ mol} \cdot \text{L}^{-1}$ EDA is shown in Fig.7a. Only one reduction peak is observed at about -0.38 V . As described above, BDO adsorbed on the surface of WE and EDA forms new complex with Cu^{2+} ions. Both the addition of BDO or EDA will decrease the overpotential for Cu deposition. In the presence of BDO and EDA the reduction potential of Cu^{2+} still shifts positively compared to that of electrolyte without additives, indicating that the presence of BDO and EDA is favorable for deposition of Cu. However, a negative shift in the reduction potential is observed compared to that of electrolyte containing $0.003 \text{ mol} \cdot$

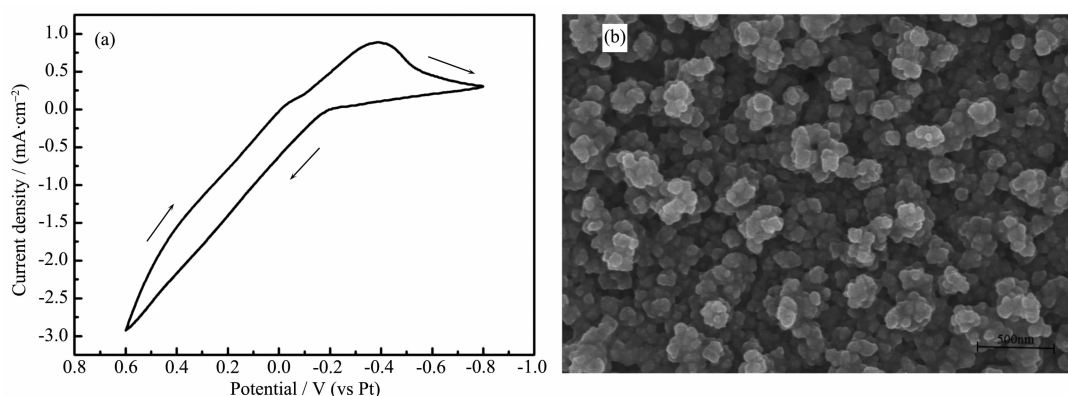


Fig.7 (a) CV on Cu WE in [HMIM]OTF containing $0.1 \text{ mol} \cdot \text{L}^{-1} \text{ Cu}(\text{CF}_3\text{SO}_3)_2$ with $0.003 \text{ mol} \cdot \text{L}^{-1}$ BDO and $0.003 \text{ mol} \cdot \text{L}^{-1}$ EDA; (b) SEM images of the electrodeposits obtained by a potentiostatic electrolysis on Cu substrate in [HMIM]OTF containing $0.1 \text{ mol} \cdot \text{L}^{-1} \text{ Cu}(\text{CF}_3\text{SO}_3)_2$ with $0.003 \text{ mol} \cdot \text{L}^{-1}$ BDO and $0.003 \text{ mol} \cdot \text{L}^{-1}$ EDA

L^{-1} BDO or $0.003 \text{ mol} \cdot \text{L}^{-1}$ EDA, suggesting that a repulsive interaction might exist between BDO and EDA: (a) the addition of EDA may suppress adsorption of BDO; (b) the adsorption of BDO on the surface of WE may inhibit the reduction process of the newly formed complex. Thus, the reduction potential of Cu^{2+} moves negatively compared to that of electrolyte containing $0.003 \text{ mol} \cdot \text{L}^{-1}$ BDO or $0.003 \text{ mol} \cdot \text{L}^{-1}$ EDA.

After a potentiostatic electrolysis at -0.4 V for 2 h, a bright Cu film is obtained. Fig.7b presents the surface morphology of deposited Cu with the addition of BDO and EDA. Nano-sized Grains are obtained and the deposit is more granular than that of the Cu surface obtained without additives.

3 Conclusions

In the present work, the effect of addition on electrodeposition of Cu from [HMIM]OTF has been studied. Due to higher adsorbing ability, the BDO is adsorbed on the surface of the working electrode instead that of HMIM^+ , which makes the deposition potential of Cu^{2+} ions shifted to more positive side., The addition of BDO, even though at a very low concentration, alters the morphology of electrodeposits effectively. The surface morphology of the deposit obtained with BDO is more granular and smoother than that of the deposit without BDO.

In the presence of EDA, the coordination

environment of Cu^{2+} is changed and the deposition potential of Cu^{2+} shifts to positive side, which is due to the formation of new complex with positive charge. The surface morphology of deposit is flatter than that without EDA since the newly formed complex is expected to be more stable thermodynamically than that formed by Cu^{2+} and CF_3SO_3^- .

When BDO and EDA are added into [HMIM]OTF at the same time, the reduction potential of Cu^{2+} still shifts positively compared to that obtained without additives. When compared to that of Cu obtained with BDO or EDA a negative shift is observed, which may be caused by a repulsive interaction between BDO and EDA. The surface morphology of the obtained deposit is more granular and nano-sized grains are obtained.

Acknowledgment: This work is supported by National Nature Science Foundation of China(No. 51074057).

References:

- [1] Endres F. *ChemPhysChem*, **2002**,**3**:144-154
- [2] Abbott A P, McKenzie K J. *Phys. Chem. Chem. Phys.*, **2006**,**8**:4265-4279
- [3] Armand M, Endres F, MacFarlane D R, et al. *Nat. Mater.*, **2009**,**8**:621-629
- [4] Endres F, MacFarlane D, Abbott A P. *Electrodeposition from Ionic Liquid*. Weinheim: Wiley-VCH, **2008**.
- [5] Hsieh Y T, Leong T I, Huang C C, et al. *Chem. Commun.*,

- 2010,46**:484-486
- [6] Hsieh Y T, Sun I W. *J. Electrochem. Commun.*, **2011,13**: 1510-1513
- [7] Zein El Abedin S, Giridhar P, Schwab P, et al. *J. Electrochem. Commun.*, **2010,12**:1084-1086
- [8] Gasparotto L H S, Borisenko N, Bocchi N, et al. *Phys. Chem. Chem. Phys.*, **2009,11**:11140-11145
- [9] Shimamura O, Yoshimoto N, Matsumoto M, et al. *J. Power Sources*, **2011,3**:1586-1588
- [10] Kornyshev A A. *J. Phys. Chem. B*, **2007,111**:5545-5557
- [11] Fedorov M V, Kornyshev A A. *J. Phys. Chem. B*, **2008,112**: 11868-11872
- [12] Abbott A P, Barron J C, Frisch G, et al. *J. Electrochimica Acta*, **2011,56**:5272-5279
- [13] Fukui R, Katayama Y, Miura T. *J. Electrochimica Acta*, **2011,56**:1190-1196
- [14] Abbott A P, El Ttaib K, Frisch G, et al. *Phys. Chem. Chem. Phys.*, **2009,11**:4269-4277
- [15] Cerisier M, Attenborough K, Fransær J, et al. *J. Electrochem. Soc.*, **1999,146**:2156-2162
- [16] Grujicic D, Pesic B. *J. Electrochimica Acta*, **2002,47**:2901-2912
- [17] Donepudi V S, Venkatachalapathy R, Ozemoyah P O, et al. *Solid State Lett.*, **2001,4**:C13-C16
- [18] LI Ya-Bing(李亚冰), WANG Wei(王为), LI Yong-Lei(李永磊). *Chinese J. Inorg. Chem.*(无机化学学报), **2008,24**(4): 534-540
- [19] YANG Rui-Na(杨瑞娜), HU Xiao-Yuan(胡晓院), DUAN Zheng(段征), et al. *Chinese J. Inorg. Chem.*(无机化学学报), **1999,15**(6):697-708
- [20] Gu C D, You Y H, Wang X L, et al. *Surface & Coatings Technology*, **2012,209**:117-123
- [21] Chen P Y, Deng M J, Zhuang D X. *J. Electrochimica Acta*, **2009,54**:6935-6940
- [22] Sakamoto T, Azumi K, Tachikawa H, et al. *J. Electrochimica Acta*, **2010,55**:8570-8578
- [23] Katayama Y, Fukui R, Miura T. *J. Electrochem. Soc.*, **2007, 154**:D534-D537
- [24] Rodriguez-Torres I, Valentin G, Lapique F. *J. Appl. Electrochem.*, **1999,29**:1035-1044
- [25] Zhu Y L, Kozuma Y, Katayama Y, et al. *J. Electrochimica Acta*, **2009,54**:7502-7506
- [26] Valencia H, Kohyama M, Tanaka S, et al. *J. Chem. Phys.*, **2009,131**:244705(1)-244705(11)
- [27] FANG Jing-Li(方景礼). *Theory and Applications of Electroplating Additives* (电镀添加剂理论与应用). Beijing: National Defense Industry Press, **2006**.